TURBULENT FLOW IN A CLOSED COMPOUND CHANNLES

J. N. V. Goulart, jg@mecanica.ufrgs.br
S. V. Möller, svmoller@.ufrgs.br
PROMEC – Universidade Federal do Rio Grande do Sul
Rua Sarmento Leite, 425 – Porto Alegre – Rio Grande do Sul – Brasil
Porto Alegre – Rio Grande do Sul, Brasil
cep: 90050 – 170

Abstract. *Experimental technique was used in order to know features of the spatial developing mixing layer, generated by two different kinds of compound channels. The first one consist in two rectangular tubes attached on a side wall of a wind channel apart from one each other by a distance "d", forming a narrow gap. Second compound channel is formed by the same tubes, but this time attached on the top and bottom walls of the wind channel, building two main channels connected by a narrow gap with width "d". The geometrical characteristics of these channels generate velocity profiles with very high vorticity values, which may give rise to large scale structures with periodical characteristics. The working fluid is air. Eight different configurations were studied. Results allow a developing mixing layer in both configurations and Strouhal numbers around 0.15.*

Keywords*: compound channels, coherent structures, hot wires*

1. INTRODUCTION

Compound channels are characterized by the presence of a narrow region connecting two main channels, like in rod bundles of nuclear reactors, where two adjacent subchannels are connected by the narrow gap between the rods, Möller (1991). As remarkable features of these kinds of channels are the unusual Reynolds stresses distribution and the sinusoidal patterns of the velocities series taken from these channels, as well. Being these facts very well reported by Knight and Shiono (1990), Soldini et al. (2004), when the authors studied open compound channels. Related to closed compound channels the works from Möller (1991), Meyer and Rehme (1994) and Meyer and Rehme (1995), showed the same features found in open channels.

Despite unusual Reynolds stresses distribution, the main source of interest has being turned on sinusoidal patterns of velocity fluctuations due to its potential ability to turn into an important source of disturbances in the flow. Flow pulsations in rod bundles were first reported by Rowe et al. (1974), where the axial component of the velocity fluctuation presented periodical characteristics. The frequency associated to this phenomenon increased when the distance between the rods was reduced. Möller (1991), employed hot wire anemometry to determine the origin and characteristics of this phenomenon. The results demonstrated that the flow pulsations were associated to the strong vorticity field near the gaps and that the dimensionless frequency in form of a Strouhal number was a function of the geometry of the channel. The Strouhal number was defined with the rod diameter and the friction velocity in the narrow gap between the rods.

Quasi-periodical flow pulsations were also found in other kind of compound channel, showing this phenomenon was not restricted to rod bundles assembly. Wu and Trupp (1994), performed hot wire measurements in a trapezoidal channel containing a single tube. The results showed pronounced peaks in spectra, confirming the strong dependence of the frequency on geometrical parameters and the flow velocity. After that, Meyer and Rehme (1994) and Meyer and Rehme 1995, performed measurements in unusual compound channels. By using hot wire anemometry, the authors studied the flow characteristics in a channel with two or several parallel plates attached to a wall in geometry similar to an internally finned channel, so that one or more narrow channels were connected to a wider one, and in a test section formed by two rectangular channels connected by a slot. The parallel plates geometry had values of the geometrical parameter $d/g = 1.66$ to $d/g = 10.0$, being "d" the depth of the slot formed by the plates and "g" the distance between two plates. Authors observed the presence of large scale structures producing flow pulsations for $d/g \geq 2$ confirmed by flow visualizations experiments for Reynolds numbers as low as Re = 150. A correlation for the Strouhal number was proposed based on the velocity measured in the edge of the plates, and the square root of the product of "d" and "g", but the results showed discrepancies for d/g values greater than 7.

One of the tree compound channels studied by Meyer and Rehme (1995), was also investigated by Goulart and Möller (2006) and Goulart and Möller (2007). In the first work (Goulart and Möller, 2006), the authors investigated a rectangular channel with two parallel plates attached on the lateral wall. By using hot wires were performed measurements of two components of velocities for six test sections where depth-width ratio remained constant $d/g = 5$. Test sections were divided into 2 groups, in the first one, all geometrical parameters, "d", "g", and "x", being "x" the length of test section, were chosen in order to keep constant any kind of geometrical ratio that can be described, eg. d/g, x/d, x/g or x/(gd)0.5 . In the second group, only d/g ratio was kept constant.

Despite the findings reported by Meyer and Rehme (1995), large-scale structures could not be found in all test sections belonging to the first group, but only in the test section with the smallest width, "g". This work led to a second investigation that showed the strong relationship between axial velocities profiles and the presence of large-scales structures. In Goulart and Möller (2007), the authors were succeeded in obtaining comprehensive measurements of the axial and transversal velocities fluctuations in ten test sections, involving three d/g ratios, 5, 10 and 12.50. The results showed a steady state plane turbulent mixing layer in spatial development between the plates. By using self-similarity functions it was possible to describe mean axial velocity (at the symmetry lines) as a tangent hyperbolic function. As regard flow large-scales appearances, velocity and length scales for a Strouhal number definition were defined. The Strouhal number defined with mixing layer thickness, $\delta_{(x)}$, and the convection velocity, U_c, remained constant even for the deepest test section, where d/g = 12.50.

Again, attention is focused on overall features of the developing mixing layer in two sorts of compound channels. The first one concerns to a rectangular main channel connected to a narrow gap. In the second part, the main channel was splitted and two main channels connected by a gap are formed. The second part of this work is also an attempt to develop a methodology for handling problems involving rod bundles assemblies.

2. TEST SECTION AND EXPERIEMTNAL TECHNIQUE

The test section, Fig. 1, consists in a 3320 mm long channel where both width, “W”, and height, “H”, are variable. While dimension “H”, is increased in the range of 54 to 60 (mm), three different values, for “W”, were adopted, namely 75, 120 and 130 mm. A splitter plate was placed along of its longitudinal dimension to reduce the height of the wind channel, Fig. 1 (a). Working fluid was air at room temperature, driven by a centrifugal blower controlled by a frequency inverter, reaching the test section with about 1% turbulence intensity. A Pitot tube, placed on a fixed position upstream of the test section, was used to measure the reference velocity U_{ref} of the experiments that was remained almost constant.

Inside the channel two different topologies of compound channels were built. In the first one, two rectangular aluminium bars with thickness e = 1.2 mm and length “L” were attached on a side wall of the wind channel, Fig. 1(b). Main dimensions are the depth “p” and width “d”. Another topology consists in moving these bars towards the center of the channel forming two subchannels connected by a central gap with same width and depth, “d” and “p”, respectively, Fig. 1 (d). Coordinates system is placed as shown in Fig 1 (e) and (f).

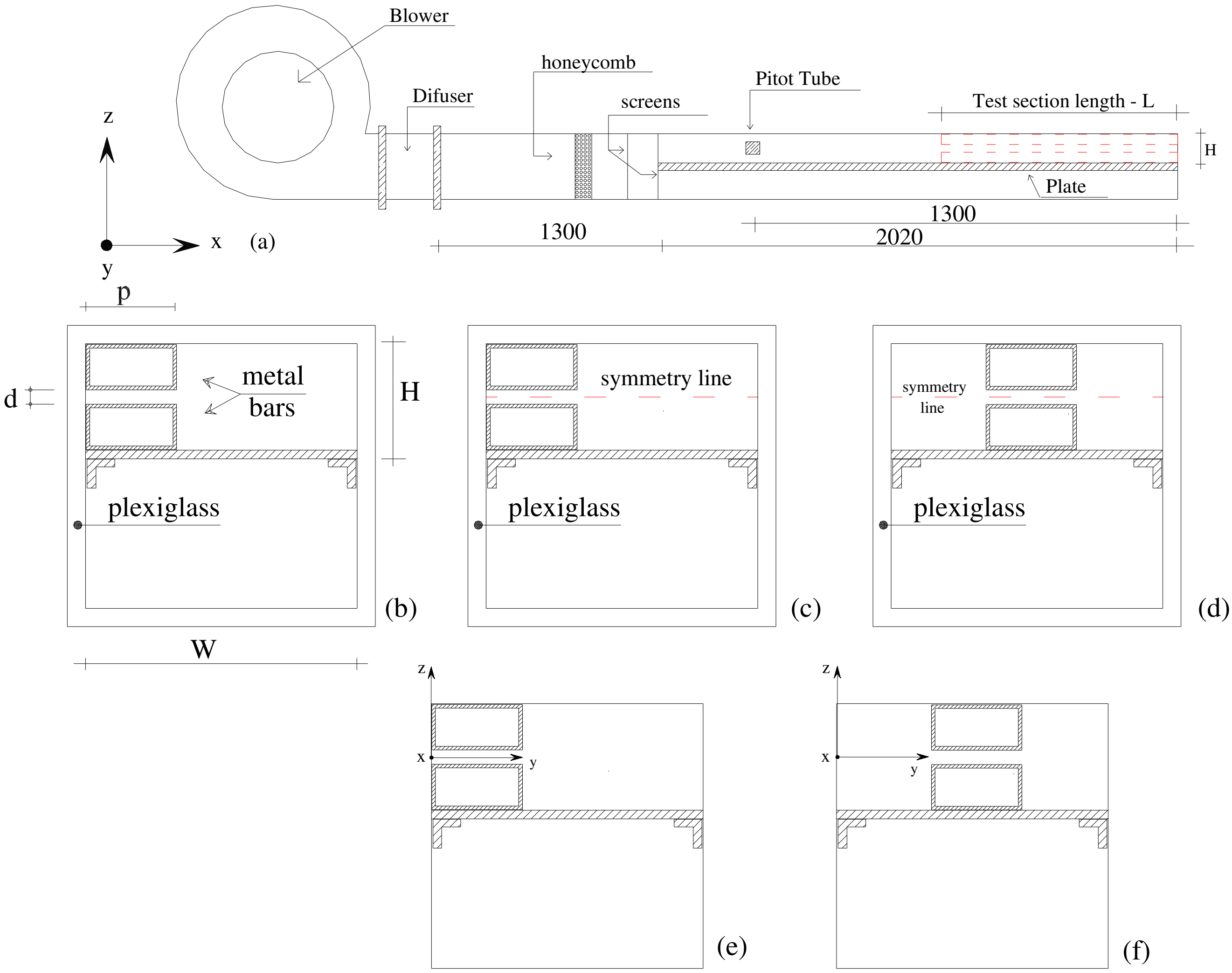

Figure 1 – Schematic view of the test section. Cross-section and coordinate system for each test section configuration.

The first topology will be called, thereafter, “SS” and the second “DS”. These names are suitable, in the first case there is only one main subchannel (single-subchannel), and in the second case, there are two main subchannels (double-subchannel).

Four different configurations were investigated for each topology, “Tab. 1”. By working with the same concepts used in the previous paper, Goulart and Möller (2007), Reynolds numbers were defined using as velocity scale the difference between upper and lower velocities measured in the border of the mixing layer and as length scale, the mixing layer thickness, $\delta_{(x)}$. This definition is very usual in problems involving open compound channels, and, seemingly, provides a better comprehension of the flow. Using the criteria adopted, the experiments were performed within Reynolds number from 5.12×10^3 up to 16.00×10^3 .

Table 1 – Test section configurations and Reynolds number – (Dimensions in mm).

Test section #	w	p	d	L	p/d	w/p	U_{ref} m/s	$Re = \dfrac{\Delta U \times \delta_{(x)}}{\nu}$
SS-01	130	50	10	1250	5.00	2.60	13.20	14.20×10^3
SS-02	130	50	4	1250	12.50	2.60	13.25	16.00×10^3
SS-03	120	38	4	1000	9.50	3.15	13.15	8.00×10^3
SS-04	75	25	4	500	6.25	3.00	13.22	8.05×10^3
DS-05	130	50	10	1250	5.00	2.60	13.20	11.99×10^3
DS-06	130	50	4	1250	12.50	2.60	13.26	12.76×10^3
DS-07	120	38	4	1000	9.50	3.15	13.14	11.49×10^3
DS-08	75	25	4	500	6.25	3.00	13.15	5.12×10^3

Measurements of velocity and velocity fluctuations were performed by a hot wire DANTEC StreamLine system using a double wire probe with a slant wire (45^o) and a wire perpendicular to the main flow to perform simultaneous measurements of the transversal (y – parallel to the symmetry line, Fig. 1 (c) and (d)) and axial components (u) of the velocity vector. All measurements were performed 20 mm upstream of the channel outlet.

Collis and Williams (1959), method with modifications by Olinto and Möller (2004), was applied for the evaluation of the anemometer signals. Velocity field was previously measured by a Pitot tube.

Data acquisition was performed by means of a 16 bit National Instruments NI USB – 9162 A/D converter board, with a sampling frequency of 3 KHz and a low pass filter set at 1 KHz. Temporal series were 43.69 s long.

3. RESULTS AND DISCUSSION

3.1. Velocity profile

Figure 2 (a) and (b), presents the velocity distribution along the symmetry line of SS-01, “Table 1”, as well as, a 3D-plot of mean axial velocity field in the main channel. Mean axial velocity and coordinates are not dimensionless. Both pictures are in good agreement with those presented in Meyer and Rehme (1994), who reported, in the same channel configuration flow acceleration towards the main channel followed by a velocity reduction in the narrow gap. Previous research has been treated this kind of flow as a bounded spatial developing mixing layer beginning at the narrow gap region and extending towards the main channel (Goulart and Möller, 2007). Being this sort of flow distribution usually found in this kind of compound channel.

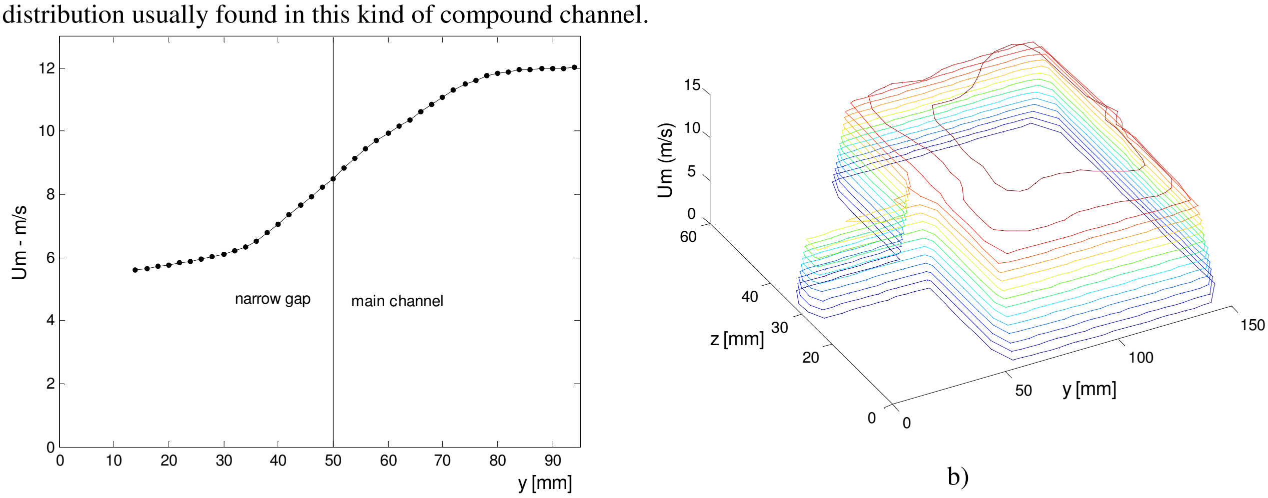

a) b)

Figure 2 – Axial velocity distribution – SS-01. (a) mean axial velocity profile. (b) 3-D – plot of mean axial velocity field.

Mixing layer are characterized by the presence of two mains streams with different velocities, the highest one, U_2, and the lower, U_1. Between them, the velocity profile can be established as a function of the self-similarity proprieties. In bounded mixing layers, generated by a narrow gap, the wall influence is important for U_1 evaluation, being necessary to determine the position where wall influence ends and the beginning of the shear layer. This is the location of the lower velocity U_1. Related to the upper velocity, U_2, its evaluation is not a hard task, since is the highest mean axial velocity on the profile. Figure 3 presents how mean axial velocity profile was divided: at the zone 1, the velocity profile suffers from wall influence, while zone 2 represents the mixing layer itself.

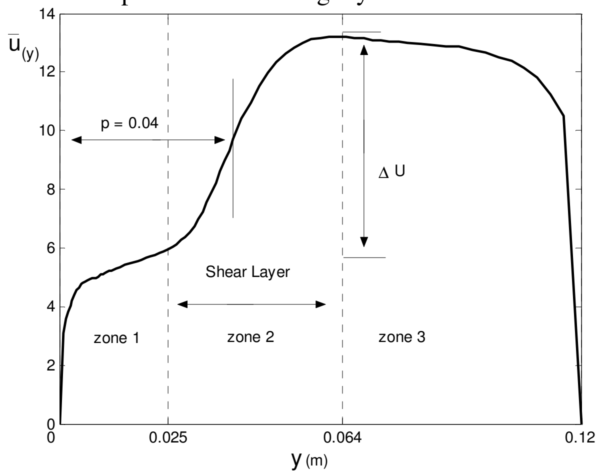

Figure 3 – Axial velocity profile on symmetry line of a compound channel. Goulart and Möller (2007).

The lower velocity, U_1, is defined as the velocity value where the velocity gradient changes its concavity, then, at this position,

$$\left.\frac{\partial^2 \overline{u}}{\partial y^2}\right|_{y_1} = 0 \tag{1}$$

By following this brief review about bounded mixing layers in compound channels, it is expected the two main channels connected by the same narrow gap topology, give rise two mixing layers on both sides of the narrow gaps.

Mean axial velocity profile and its gradient, from test section DS-04, are presented in Fig. 4 (a) and (b). Both are measured on the symmetry line being depicted as a y-axis function.

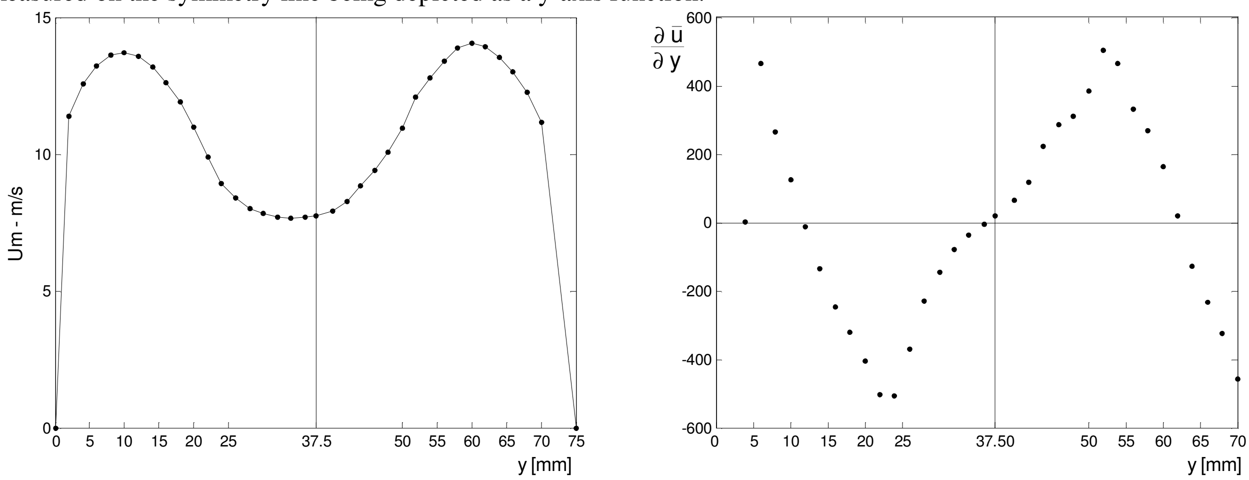

a) b)

Figure 4 – Mean axial velocity profiles on each side of the narrow gap and their gradients, (a) and (b), respectively.

The solid line on Figure 4 (a) shows the central gap reference and as predicted, two mixing layers are formed in both sides of the channel. Therefore, a small difference between both sides can be observed, showing entrance effects are still present. Another remarkable feature concerns to the position where U_1 takes place. In this kind of configuration, the upper velocity of the mixing layer, U_2, occurs in the main channels (both sides), while lower velocity, U_1, can be found near the central position of the gap. Therefore, the wall of the channel no longer affects the flow, since there is no wall in the gap, being, U_1, directly inferred. Figure 4 (b) shows the derivative of the axial velocity profile ($\partial u / \partial y$). At the centers of mixing layers derivative shows its highest value (almost the same values on both sides), on the other hand, at the center of the gap its value is null.

Although, all test section studied show the same characteristic related to mean axial flow distribution along the symmetry line, the symmetry of the velocity profiles was not achieved for all test sections in the "DS" configuration. Being this result depicted in Fig. 5 (a). The start and end points of the measurements are 14 mm away form the each lateral wall. On the right side of the channel the velocity profile shows its maximum values, and starts to decrease affected by the lateral wall. On the left side, the same does not occur, the maximum value of velocity was not attained, at this distance.

Figure 5 (b) shows a 3D-plot of axial velocity field. Velocity distribution is very similar to that found in Figure 2 (b) where only one mixing layer was produced.

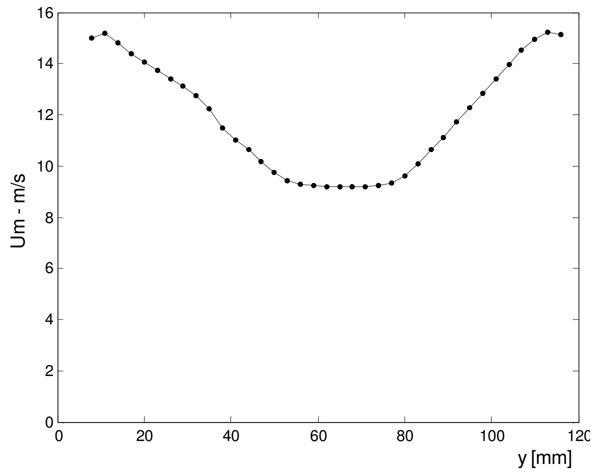

a)

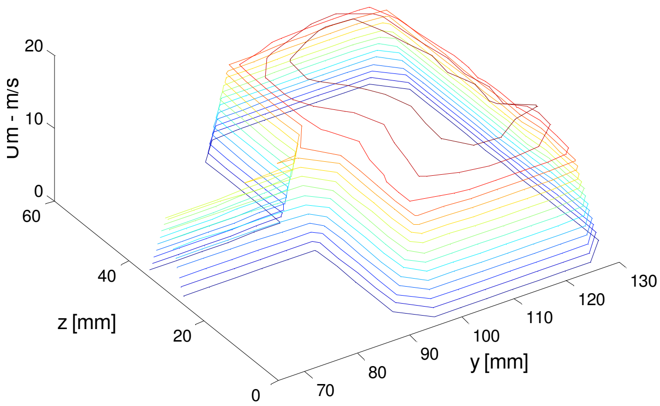

b)

Figure 5 – Mean axial velocity measurements in DS-05. a) velocity profile. b) mean axial velocity field.

3.2. Velocity distribution in mixing layers

As observed, it is possible to describe this problem as a steady state plane turbulent mixing layer in spatial development, and its two dimensional form can be written as follow,

$$\bar{u}\frac{\partial \bar{u}}{\partial x}+\bar{v}\frac{\partial \bar{u}}{\partial y}+\frac{\partial \overline{u'v'}}{\partial y}=\nu\frac{\partial^2 \bar{u}}{\partial y^2} \tag{2}$$

where $\bar{u}$, $\bar{v}$, are axial and transversal velocity components respectively and ν is the molecular (kinematic) viscosity. Being, $\overline{u'v'}$, shear stresses caused by velocity fluctuation.

According to Lesieur (1997), the self-similar solution for the Eq. (2), leads to an error function for the mixing layer velocity profile, however, a hyperbolic tangent function (tanh) is widely used as an approximation, thus

$$\bar{u}(\eta) = U_c + \frac{\Delta U}{2}\tanh(\eta) \tag{3}$$

where:

ΔU = difference between the lower and the upper velocities in the mixing layer, U_1 and U_2, respectively;

U_c = convection velocity, defined by

$$U_c = \frac{U_2 + U_1}{2} \tag{4}$$

η = similarity parameter, Prooijen and Uijttewaal (2002), have defined as

$$\eta = 2\sigma\frac{y - y_c}{X} \tag{5}$$

where

y_c = coordinate of the center of the mixing layer;

X = downstream distance where the axial velocity profile were obtained;

σ = inverse of mixing layer thickness growth

$$\sigma = \frac{X}{\delta_{(x)}} \tag{6}$$

$$\delta_{(x)} = \frac{U_2 - U_1}{\left.\frac{\partial \bar{u}}{\partial y}\right|_{max.}} \tag{7}$$

Figure 6 (a) and (b) show the velocity profiles of test sections SS-02 and DS-07 (right side for the last one). Experimental data were plotted as a function of the similarity parameter η, and fitted by using Eq. (8)

$$U_{ad} = 2\frac{\bar{u}(\eta) - U_c}{\Delta U} = \tanh(\eta) \tag{8}$$

Indeed, the hyperbolic tangent function presented a good agreement with experimental data, for all cases investigated. Therefore, some discrepancies were found, mainly at the edges of the profiles.

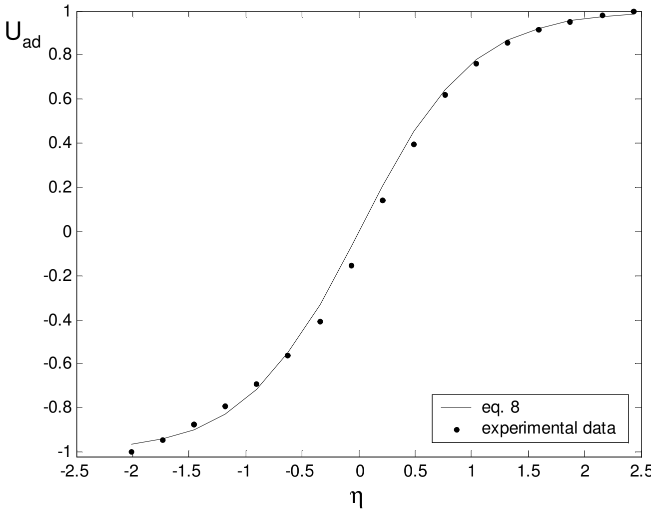

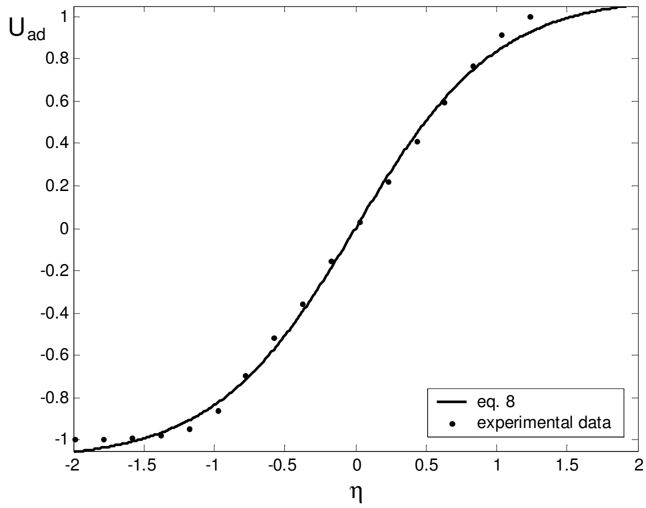

Figure 6 – Mean axial velocity distribution in the mixing layer and its approximation by hyperbolic tangent function. a) SS-02. b) DS-07.

Since self-similarity is attained, flow quantities are only dependent on local variables, including mean velocities, its fluctuations, and the local length scale, mixing layer thickness, δ. In theory, it is expected a linear mixing layer growing with the streamwise coordinate in the self-similar state. Figure 7, shows the width of shear layer as a function of section test length "X", for both configurations. Width of the shear layer was obtained by using Eq. (7). Despite the scattering of the data, a linear fit seems to be adequate for the data from first configuration, SS, curve "A". Nevertheless, data from second configuration DS, cannot be fitted by linear approach. Non-linear dependence between mixing layer thickness and streamwise distance may suggest that the self-similar state has not been attained for all test sections in this configuration.

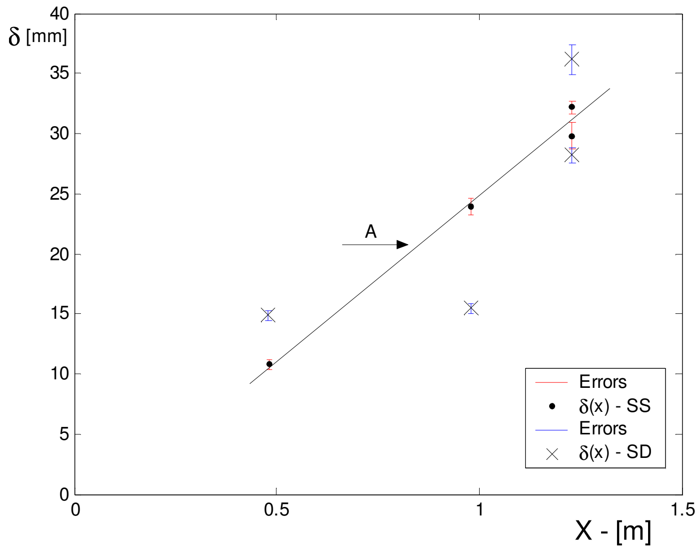

Figure 7 – Mixing layer growth as downstream distance function.

3.3. Reynolds stresses distribution

The profiles for the Reynolds normal stresses ($\overline{u'^2}$, $\overline{v'^2}$) and the shear stress, $\overline{u'v'}$, are presented in Fig. 8 and Fig. 9(a) and (b), being the values, presented as dimensionless form by using the velocity difference (U_2 - U_1). As regards Fig. 8, this one shows these values as a function of self-similarity coordinate. The normal Reynolds stresses and the shear stress distributions showed the same behavior for all cases, reaching the maximum value at the center of mixing layer, $\eta = 0$, (edge of the narrow gap), decreasing quickly towards the main channel.

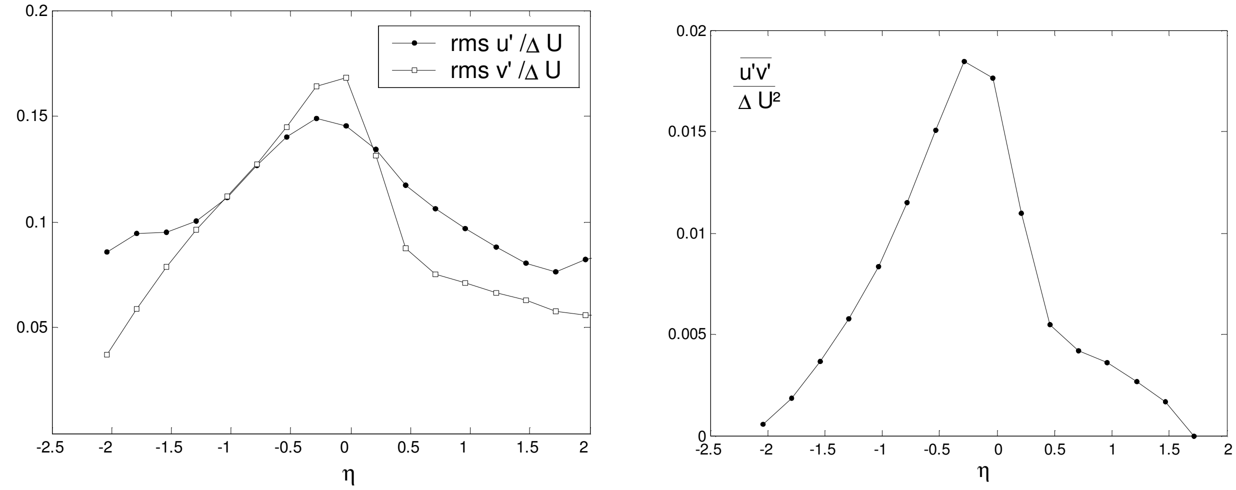

a) b)

Figure 8 – Profiles of normal Reynolds stresses and shear stress, on the symmetry line, test section SS-03.

Figure 9 (a) and (b), show normal Reynolds stresses and shear stress quantities in the second configuration, DS, as a y-distance function.

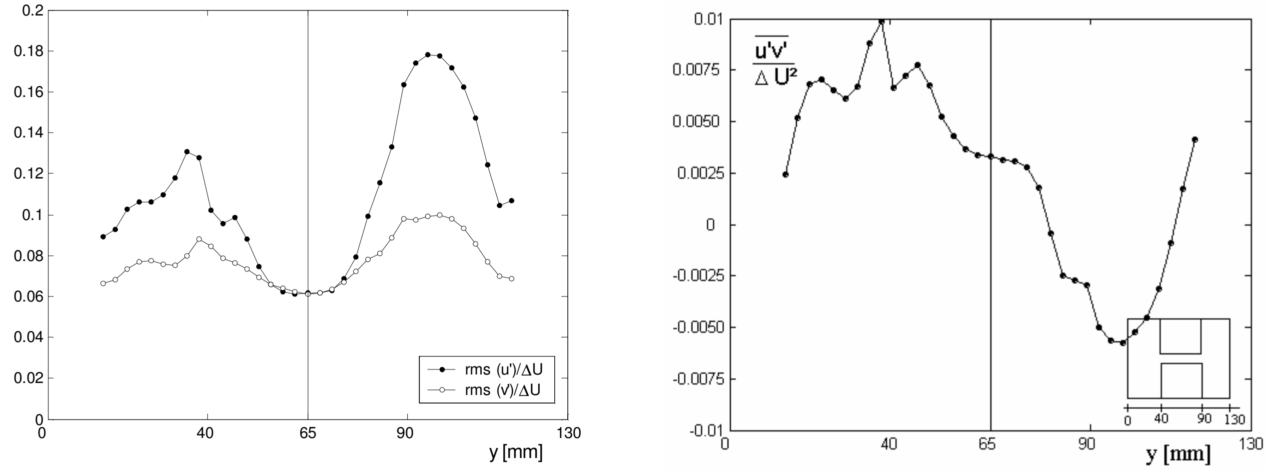

a) b)

Figure 9 - Profiles of normal Reynolds stresses and shear stress on the symmetry line, test section DS – 08

As expected, peaks of normal Reynolds stresses and shear stress appear on the both sides of narrow gap. These ones are produced by two developing mixing layers, as mentioned before. With exception of test section DS – 08, the lack of symmetry was almost typical characteristic for "DS" configurations. Another noteworthy feature is related to the opposite signs of shear stress peaks on the right and left sides of the narrow gap, Fig. 9 (b). This fact is already expected, here two strong vortical fields are formed on the each side of the gap, and such as predicted by Möller (1991), these fields have opposite signs.

Investigations on coherent structures in the flow were also performed, for test sections SS - 02 and DS - 06. Figure 10 (a) and (b), show autospectral density functions for both velocity fluctuations components, u' and v', being $\Phi_{uu} = \Phi_{vv} = \frac{m^2}{s^2} Hz$. Both records of velocities were taken at the same position inside the mixing layer, η = -0.33. When the frequencies are analyzed, a lower frequency is observed in the first graph (left side), around 35Hz , when compared to that one stressed on the second graph, around 50 Hz. A dimensionless form for Strouhal numbers was studied by Goulart and Möller (2007), the authors showed that mixing layer thickness, $\delta_{(x)}$, and convection velocity, U_c, were very suitable scales for Strouhal numbers in this kind of compound channels

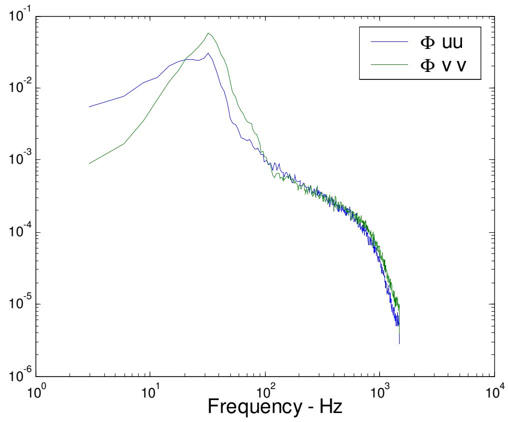

a)

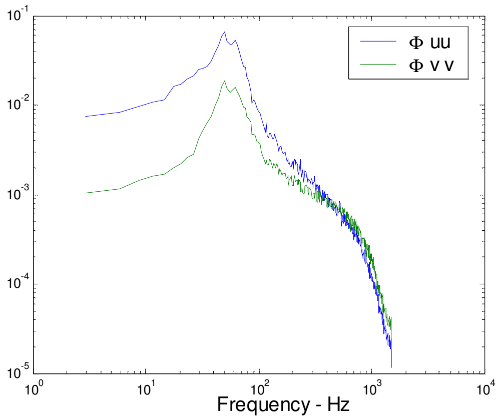

b)

Figure 10 – Autospectral densities. a) test section SS-02. b) test section DS – 06.

In fact, by using the respective scales (from each test section), both Strouhal numbers were ranged in 0.15. The first case, $St_{ss} = 0.148$ and the second $St_{DS} = 0.145$. Being these values a little bit lower than those measured in Goulart and Möller (2007), who found St = 0.17.

4. CONCLIDING REMARKS

In this paper, an experimental study of mean and fluctuating velocities of the turbulent flow in two sorts of compound channels was performed. The main purpose was the investigation of the flow characteristics in these two different channels and an attempt to describe mean quantities as self-similarity functions, such as done in a previous paper, Goulart and Möller (2007).

The results of the velocity measurements showed the presence of a shear layer in both configurations investigated. The mean and fluctuating quantities distribution reminded as self similarity function, showing the self preserving characteristics of the flow. Therefore, for DS configuration test sections, entrance effects were still present, being this fact pointed by asymmetrical behavior of mean quantities profile, on the symmetry line.

Spectral investigations, by means of Strouhal number, defined with the main frequency component of the velocity fluctuation, the convection velocity and the shear layer thickness. Although, the Strouhal number, as defined, have led to good results, lower values than those generated by two plates, Str=0.17, were obtained. Therefore, the discrepancy between Strouhal numbers in axial and transversal velocity components was not found.

5. ACKNOWLEGMENTS

The support by the CNPq – Brazilian Scientifical and Technological Council is grateful acknowledged.

Jhon N. V. Goulart thanks also the CNPq for granting him a fellowship.

6. REFERENCES

Collis, D. C. and Willans, M. J., 1959, Two-dimensional convection from heated wires at low Reynolds numbers, J. Fluid Mech., 6, 357-384.

Goulart, J. N. V. and Möller, S. V., 2006, Flow pulsations in short compound channels. In: 11º Congresso Brasileiro de Engenharia e Ciências Térmicas - ENCIT, 2006, Coritiba, 2006.

Goulart, J. N. V. and Möller, S. V., 2007, Shear flow in compound channels. In: 19º International Congress of Mecahnical Engeneering - COBEM, 2007, Brasilia, 2007.

Knight, D.W. and Shiono, K., 1990, Turbulence measurements in a shear-layer region of a compound channel, Journal of Hydraulic Research, 28, 175-196.

Lesieur, M., Turbulence in Fluids. Third Edition, Kluwer Academic Publishers, Dordrecht, The Netherlands.

Meyer, L. and Rehme, K., 1994, Large-scale turbulence phenomena in compound rectangular channels, Experimental Thermal and Fluid Science, 8, 286-304.

Meyer, L. and Rehme, K., 1995, Periodic vortices in flow though channels with longitudinal slots or fins, 10th Symposium on Turbulent Shear Flows, The Pennsylvania State University, University Park, August 14-16.

Möller, S. V., 1991, On Phenomena of Turbulent Flow through Rod Bundles. Experimental Thermal and Fluid Science, 4, 25-35.

Olinto, C. R. and Möller, S. V., 2004, X-probe calibration using Collis and William's equation. In: 10º Congresso Brasileiro de Engenharia e Ciências Térmicas - ENCIT, 2004, Rio de Janeiro, 2004.

Prooijen, B. C. van and Uijttewaal, W. S. J., 2002, A linear approach for the evolution of coherent structures in shallow mixing layers, Physics of Fluids, 14, 4105-4114.

Rowe, D.S., Johnson, B.M. and Knudsen, J. G., 1974, Implications concerning rod bundle crossflow mixing based on measurements of turbulent flow structure, Int. J. Heat Mass Transfer, 17, 407-419.

Soldini, L., Piattella, A., Brocchini, M., Mancinelli, A. e Bernetti, R., 2004, Macrovortices-induced horizontal mixing in compound channels, Ocean Dynamics, 54, 333 – 339.

Townsend, A. A., 1976, The structure of turbulent shear flow. Cambridge University Press, Cambridge, England, 188-230.

Wu, X. and Trupp, A. C., 1994, Spectral measurements and mixing correlations in a simulated rod bundle subchannels, Int. J. Heat Transfer, 37, 1277-1281.

7. RESPONSIBILITY NOTICE

The authors are the only responsible for the printed material included in this paper.